

# NMR and Bayesian regularized neural network regression for impurity determination of 4-aminophenol

Jenny Forshed<sup>a</sup>, Fredrik O. Andersson<sup>b</sup>, Sven P. Jacobsson<sup>a,b,\*</sup>

<sup>a</sup> Department of Analytical Chemistry, Stockholm University, SE-106 91 Stockholm, Sweden

<sup>b</sup> Analytical Development, Pharmaceutical and Analytical R&D, AstraZeneca R&D, SE-151 85 Sodertalje, Sweden

Received 19 December 2001; received in revised form 13 February 2002; accepted 1 March 2002

## Abstract

A method for the determination of 4-aminophenol as an impurity in paracetamol (*N*-(4-hydroxyphenyl)-acetamide) by proton nuclear magnetic resonance (<sup>1</sup>H-NMR) spectroscopy has been developed. The <sup>13</sup>C-satellite from the protons in the *ortho* position from the hydroxyl group in paracetamol was used as an internal standard, although these peaks interfered with the peaks from the protons in 4-aminophenol. Because of interference in the spectra and non-linearity over a wide calibration range, a Bayesian regularized neural network model was used for calibration. Various kinds of data preprocessing were examined: zero filling, multiplication by a negative exponential function (line broadening), followed by Fourier transformation of the free induction decay (FID). The NMR spectral data were automatically phased and shift-adjusted by means of a genetic algorithm. Multiplicative scatter correction and data compression by wavelets and sequential zeroing of weights variable selection were performed to obtain an optimal calibration model. Neither zero filling of the FID nor line broadening improved the calibration models with regard to error of prediction, so these processes were excluded in the final model. The generated Bayesian regularized neural network model was evaluated with an independent test set. Four different models with different test sets were constructed to explore the quality of the calibration. The mean error of the optimal calibration model was  $25.3 \times 10^{-6}$  weight of 4-aminophenol per weight paracetamol. The method is characterized by being relative fast, simple and sufficient sensitive for typical pharmaceutical impurity determinations. © 2002 Elsevier Science B.V. All rights reserved.

**Keywords:** Quantitative nuclear magnetic resonance; Bayesian regularized neural networks; Impurity determination; 4-Aminophenol; Paracetamol

## 1. Introduction

In general, the proton nuclear magnetic resonance (<sup>1</sup>H-NMR) spectrum is very rich in information. It is structurally specific and a useful tool for both identification and quantification of organic compounds. In theory, the peak intensity of

\* Corresponding author. Tel.: +46-8-553-289-68; fax: +46-8-553-277-30.

E-mail address: [sven.jacobsson@astrazeneca.com](mailto:sven.jacobsson@astrazeneca.com) (S.P. Jacobsson).

each NMR signal exactly reflects the molar ratio of the  $^1\text{H}$  nuclei present, thus making the technique conceptually simple for quantification. Other advantages of quantitative NMR (QNMR) are its direct applicability (minimum sample preparation), its selectivity and its non-destructive nature. NMR may also give quantitative information about other potential contaminants. Compared to other analytical techniques, the major disadvantage of QNMR is its high limit of detection, a relatively large quantity of sample being required. This depends particularly on the very small differences in energy that are measured. Because organic compounds typically generate several peaks, the complexity of the spectra, especially for  $^1\text{H}$ -NMR, may also cause problems.

Early research on QNMR has been done by Hollis [1], Anhoury et al. [2], O'Neill et al. [3], Bowen et al. [4] and Kasler [5]. QNMR has been used for absolute as well as relative quantification. In order to obtain an assay, an internal reference has to be employed. When analysing impurities, however, the relative amounts are determined. The use of  $^1\text{H}$ -NMR for impurity determination has previously been reported [6–15]. At low impurity concentrations, the interference of  $^{13}\text{C}$ -satellites may present a difficulty in case of interference.  $^{13}\text{C}$ -satellites are peaks arising from proton couplings to  $^{13}\text{C}$  for protons bound to carbon atoms. The proton signal has two  $^{13}\text{C}$ -satellites, each with the intensity of 0.55% of the area of the proton resonance. Quantification in cases of interference can be accomplished by subtracting the appropriate amount of the  $^{13}\text{C}$ -satellite from the area of the peaks of interest [14], or the problem may be handled with the aid of calibration models.

The purpose of this study was to develop a method for the determination by QNMR of 4-aminophenol, an impurity in paracetamol (*N*-(4-

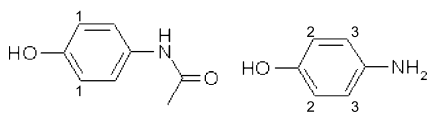


Fig. 1. Structure formula of paracetamol (left) and 4-aminophenol (right). The numbered positions are the protons involved in the calibration models.

hydroxyphenyl)-acetamide), whose structures are shown in Fig. 1. In the study, one of the  $^{13}\text{C}$ -satellites from the protons in *ortho* positions seen from the hydroxyl group in paracetamol (marked as proton 1 in Fig. 1) was used as an internal standard. Similar approaches have been reported by Lindgren [6] and Fux [13]. In the present study, the internal standard partly interfered with the peaks from 4-aminophenol. Since accurate integrations of overlapping Lorentzian shape peaks are difficult [16,17] and a nonlinear relationship was expected in a wider concentration range, because of this peak overlap, nonlinear multivariate calibration was examined.

In order to derive as suitable a method as possible, a number of NMR parameters were systematically examined, together with different methods of preprocessing the NMR data. The free induction decay (FID) was multiplied by a negative exponential function, i.e. line broadening, and zero filling of the FID was performed. After Fourier transformation, the spectra were automatically phased and shifts were aligned by means of a genetic algorithm (GA). Baseline correction was performed by multiplicative scatter correction (MSC) and spectra were compressed by means of wavelets and sequential zeroing of weights (SZW) variable selection [18].

## 2. Theory

### 2.1. NMR instrumentation

Instrumental parameters need to be carefully controlled to reduce the variance when NMR is used for quantification. Generally speaking, the stronger the field and the higher filling factor of the probe, the higher the *S/N* obtained. The filling factor is a measure of the fraction of the coil volume occupied by the sample [19]. These parameters are set by the standard set-up on the instrument and have not been optimized in this study.

The influence of the magnetic field becomes more homogeneous if the sample is spun, and this improves the signal. Good shimming, i.e. adjustment of the homogeneity of the applied

magnetic field, is also a necessity for a good  $S/N$  [20]. According to Traficante [21], a pulse angle of  $83^\circ$  and a pulse repetition period of 4.5 times the longest  $T_1$  give the optimum recovery after a pulse. Furthermore, it is a known fact that the  $S/N$  increases with the square root of the number of scans/transients. This factor has to be chosen by considering the analysis time and the required  $S/N$ .

Increasing the sample concentration and hence the number of detected nuclei increases the NMR signal and consequently the  $S/N$ . The number of detected nuclei also depends on the number of structurally equivalent nuclei in the molecule studied that give rise to one signal. Further, the appearance of the signal depends on the structural and chemical surroundings of the proton. To give an example, a singlet peak has a much higher signal-to-noise ratio than a doublet peak although they come from the same number of nuclei and thus have the same total area. This should, if possible, be considered when choosing the peak for quantification.

When analysing impurities, a weak signal has to be recorded in the presence of a strong peak from the main substance. This makes the range of the analogue to digital converter (ADC) important.

## 2.2. Data preprocessing

The signal collected by the NMR spectrophotometer is the sum total of oscillating, decaying voltages originating from magnetizations of the nuclei in the sample, each with a characteristic frequency. This is called the FID. To obtain a spectrum as a function of frequency, the FID is Fourier-transformed.

To obtain an accurate quantification with NMR, it is of considerable importance to consider the various ways of processing data. Typically, Fourier transformation of the FID, phase correction of the spectra, integration and/or calibration are required. Several other processes, e.g. line broadening and zero filling of the FID, baseline correction, shift alignment, MSC, wavelet compression and variable selection, may also be performed to improve signals and facilitate calibration modelling. In this section we will describe

these techniques briefly and will refer to the literature for further reading.

Most of the signal in the FID occurs in the first section of data points, whereas the noise should be constant throughout. Processing of the FID that emphasizes its early part should increase the  $S/N$ . The most usual way to do this is through line broadening, multiplying the FID by a negative exponential function before applying a Fourier transform [22].

The digital resolution can be improved by increasing the acquisition time and hence collecting more data points. Zero filling also increases the digital resolution through the interpolation of additional points in the spectrum. This is done by adding a string of zeroes to the end of the FID prior to Fourier transformation. This is fully described by, for example, Rabenstein and Keire [23].

Genetic algorithms (GAs), were used for automated phasing and shift alignment in this study. GAs search for the solution space of a function by simulated evolution. A GA usually starts with a random population of candidate solutions, where a string represents each solution. Each string is subjected to a genetic search, which can encompass assignment to a fitness value according to an objective function, selection of strings for further replication, recombination crossover and mutation. This genetic search runs until predefined optimization criteria are met. Comprehensive discussions of GA can be found in the literature, e.g. by Goldberg [24].

By adjusting the slope and offset of the sample spectra to the average spectrum, the chemical information is preserved while other differences between the spectra are minimized. This is called MSC and is briefly described as follows. Each spectrum is fitted to the average spectrum as closely as possible by least squares:

$$x_i = a_i + b_i m_j + e_i$$

where  $x_i$  is an individual spectrum  $i$ ,  $m_j$  the mean spectrum of the group and  $e_i$  the residual spectrum. Ideally,  $e_i$  represents the chemical information in spectrum  $i$ . The corrected spectrum,  $x_{i(\text{MSC})}$ , is calculated using the fitted constants  $a_i$  (intercept) and  $b_i$  (slope):

$$x_{i(\text{MSC})} = \frac{(x_i - a_i)}{b_i}$$

This is further described by Geladi et al. [25].

Wavelet transformation has relatively recently become a widely applied processing tool in signal processing for the efficient extraction of relevant information from spectral data, e.g. by data compression and noise reduction. Unlike Fourier transformation, which decomposes the signal into sine and cosine components of different frequencies, the wavelet transformation decomposes the signal into pieces of scaled and shifted versions of the mother wavelet [26]. The effect of the shifting and scaling process is the simultaneous appearance of a signal at multiple scales, which is called multiresolution. The wavelet thus transforms a portion of the data into different frequency components and can thereby reduce the number of variables while still preserving most of the information. In this study, discrete orthonormal wavelets are applied to NMR spectral data. The orthogonality minimizes the number of wavelet coefficients and suppresses unwanted relationships between the coefficients. This results in efficient data compression.

The variable selection method used in the present study is based on the SZW approach, in which the influence of each spectral variable is evaluated for an established neural network (NN) model. The variable influence is calculated as *rmdiff*, which is the difference in the root-mean-square error of prediction, *rmsep* (Eq. (1)), between the entire (original) model and when the weights in the NN model are zeroed to exclude one variable at the time. By means of this approach, each variable is evaluated by its contribution to the model, and a predetermined threshold can be applied to sort out the most important variables [18].

### 2.3. Calibration

Theoretically, as mentioned above, the peak intensity exactly reflects the molar ratio. If the peaks appear close to each other in the spectra, their factor of response is about the same and the molar ratios may be calculated correctly without calibration. Since the peak shapes are Lorentzian

in an NMR spectrum, an integral would have to extend to infinity in both directions in order to include all of the peak area. When the peaks appear close to each other, the range of integration, however, is limited. The integration then has to be performed in the same way on every peak of interest. This is easily done if the peaks are singlets and have no peaks immediately surrounding them. However, if the peaks are multiplets and/or interfere with each other, this is a more difficult task. A number of factors make it difficult to obtain precise NMR integrals, as has been reported in previous papers [16,17]. A calibration model may account for and handle these problems with integration and also deviations from the molar ratio.

Multilayer feed-forward NNs are utilized for nonlinear regression. NNs are composed of a highly interconnected mesh of nonlinear and linear computing elements. The fundamental processing element of a NN is the neuron. Neurons are connected by links, and there is a coefficient, a weight, associated with each link. The neurons receive external inputs or inputs from other neurons and perform a weighted sum of these inputs. The neurons process the resulting signal with a transfer function and then produce an output to other neurons or as an output from the entire model. A process known as training or learning develops the values of the weights. Starting from random values of the weights, output vectors are calculated from a set of input vectors for which the right answers are known a priori. After the calculation, an algorithm based on the differences between the output values obtained and the target values is used to modify the weights. As this process is repeated, the weights gradually converge to values that transform each input pattern to an output pattern closely conforming to its target. Any type of variation in the inputs may be accounted for by including them in the training process [27].

An important issue in developing calibration models is the validation. The purpose of the validation is to derive estimates of the accuracy of the predictions from the calibration model. A continuing validation with a training set while the model is built gives an indication of the quality of the

Table 1

The measured concentrations of the calibration solutions in ppm, weight per weight of 4-aminophenol in paracetamol

Y	B
0.0	0.0
42.2	42.1
84.7	84.1
126.3	125.3
434.1	428.8
712.9	709.6
1005.5	991.6

model, depending on the number of learning cycles in the NN training. This is critical due to the risk of overtraining. The goal of the NN training is to generate a NN that produces small errors on the training set, but will also respond properly to novel inputs.

The rmsep (Eq. (1)) was used as the error function in this work.

$$\text{rmsep} = \sqrt{\frac{\sum (y_{\text{pred}} - y_{\text{meas}})^2}{n}} \quad (1)$$

where  $y_{\text{pred}}$  is the predicted concentrations,  $y_{\text{meas}}$  is the measured concentrations and  $n$  represents the number of predictions.

The training of a feed-forward NN trained with quasi-Newton back propagation [28] is stopped when the rmsep from the validation set reaches a minimum. The training function for a Bayesian regularized artificial NN (BRANN) in this study updates the weights and bias values according to Levenberg–Marquardt optimization [27,29]. It minimizes a combination of squared errors and weights and then determines the correct combination to produce a network that generalizes well. In a standard feed-forward NN training method, single sets of parameters (weights, biases etc.) are used. The Bayesian approach to NN modelling considers all possible values of network parameters weighted by the probability of each set of weights. Bayesian regularization minimizes a linear combination of squared errors and weights. It also modifies the linear combination so that at the end of training the resulting network has a good

generalization quality [30]. The stop criterion of a Bayesian trained network is connected to the Marquardt adjustment parameter. When the parameter exceeds a maximum set value, the training is stopped [31].

A set of test samples, not included in the training process, was predicted as an independent model performance measurement, with rmsep as the error function.

### 3. Experimental section

#### 3.1. Preparation of test samples

The calibration samples were prepared in 5 mm NMR tubes by dissolving paracetamol and 4-aminophenol in DMSO- $d_6$  to the concentrations showed in Table 1. The sample with the smallest concentration of 4-aminophenol was diluted four times, and all the solutions were weighed into the samples to reach a maximal accuracy. The maximum amount of paracetamol in the samples was investigated in order to get as high an  $S/N$  ratio as possible, while avoiding overloading of the ADC. An appropriate concentration was found to be 400 mg paracetamol per ml. The calibration samples were stored in the dark in a refrigerator for up to one week. The two calibration series in Table 1 were run two times each, the runs being named Y1, Y2, B1 and B2.

#### 3.2. NMR instrumentation

The  $^1\text{H}$ -NMR spectra were recorded on a Varian UNITY spectrometer working at 400 MHz for  $^1\text{H}$  with an ASW probe and a 16-bit ADC. The samples were spinned at 20 Hz. Shims  $z$  and  $z^2$  were carefully shimmed. Pulse angle and repetition time were chosen according to Traficante [21] to be  $83^\circ$  and  $4.5 \times T_1$ , respectively, (13.5  $\mu\text{s}$  and 6.75 s for the peak from paracetamol, proton 1 in Fig. 1). The acquisition time was adequately chosen to be 2.5 s.

The oversampling factor was set at 20, which was the maximum on the NMR spectrometer used. This gave a maximum spectral width of 1250 Hz. A narrower width did not improve the

signals. A digital filter with a sharp cut-off was applied to avoid the peaks folding in. The number of points was 25 k, the maximum according to the set-up of the instrumentation. The location of the carrier frequency was investigated to give minimal disturbing effects in the spectral area of interest, while still being located as near to the peaks for quantification as possible. The number of transients/scans was preset at 200, which gave a reasonable acquisition time of about 20 min.

### 3.3. Data preprocessing

All of the mathematical processing was performed in the software MATLAB [31] Prior to the Fourier transformation, the FIDs were multiplied by a negative exponential function and zero filling to double the number of data points was performed.

By means of a GA, the spectra were automatically phased with a zero and a first-order phase correction and corrected laterally until the shifts were aligned. The fitness criterion was the sum of the differences between the actual spectrum and a manually phased spectrum. The same arbitrary number of cycles was performed for each spectrum until the differences were insignificant.

The spectral area of interest, one of the  $^{13}\text{C}$ -satellites and the 4-aminophenol signal were utilized for calibration. This part of the spectrum was treated with MSC and wavelet compressed to 162 variables, a variable reduction of 50%. In this paper, two near-symmetric wavelets, symlet 2 and symlet 8, have been employed. The name symlet denotes least-asymmetric orthogonal Daubechies wavelet. The number in the name refers to the number of coefficients necessary to define the specific wavelet. Different combinations of data pretreatment with and without zero filling, wavelet compression and line broadening were examined.

The data were preprocessed so that the input data points fell in the interval  $\{-1, 1\}$  [29]. The number of wavelet variables was reduced by variable selection by the SZW approach [18]. The NN architectures for the variable selection were a three-layer (input, hidden and output layer) feed-forward network trained with BFGS quasi-New-

ton back propagation [31]. The input neurons received the wavelet-compressed spectra as a vector. The activation function for the three neurons in the hidden layer is the sigmoid *arctan* function. The output function is linear. Fifty nets were performed and the net with smallest error, in an rmsep sense, was utilized in the variable selection [18].

### 3.4. Calibration

A Bayesian regularized NN was used to build the calibration model. The network is included in the MATLAB [31] NN toolbox and is a back propagation neural net that incorporates the Bayesian regularization algorithm for finding the optimum weights according to Levenberg–Marquardt optimization [27,29]. The architectures of the net are the same as for the variable selection described above. The variables from the variable selection were utilized to build the model.

Four calibration models were performed with partly different data. Two of the calibration series were used for building the model in the neural net for variable selection. One of the series was used as a validation set and the fourth set was excluded, this being utilized for evaluation of the final calibration model. A schematic table shows the procedures in Table 2. Rmse (Eq. (1)) was calculated and the mean error from a test set is reported as a measure of the model error.

## 4. Results and discussion

### 4.1. NMR instrumentation

When optimizing the NMR parameters it was not necessary to make the signal exactly proportional to the number of nuclei since a calibration model was constructed. The importance lay in using exactly the same instrumental parameters every run time in order to achieve as high repeatability and as high a signal as possible. The signal to noise improvement from signal averaging is proportional to the square root of number of spectra averaged. Thus, the parameters of the NMR instrumentation were chosen so as to ob-

tain a balanced compromise between signal intensity and analysis time, in this case about 20 min.

#### 4.2. Data preprocessing

Although, zero filling did improve the digital resolution visually, the error of prediction from the model with zero filling was higher than the error from the model without zero filling. Nor did line broadening improve the model's ability to predict the concentrations. The differences in error of prediction between the different models are shown in Table 3, indicating that the standard procedures in qualitative NMR are not directly transferable to QNMR procedures.

Autophasing, shift alignment, MSC, data compression by wavelets and variable selection were performed to simplify the building of the multivariate calibration model. The MSC, autophasing and shift alignments were done to minimize the

differences between spectra that did not correspond to concentration variations and to minimize instrumental variations. However, the spectral quality was adequate between experimental runs. No spectral standardization between runs to compensate for drift in instrumental parameters was required.

No significant difference in results was noticed between the two symlet wavelets symlet 2 and symlet 8. We arbitrarily chose to use symlet 2, since this is the simpler of the two. The wavelet reduction was performed in one step because this gave a sufficient number of variables for use in the variable selection process. The spectra in Fig. 2 show the appearance after autophasing and shift correction, normalization, MSC and wavelet data compression.

Fifty independent NNs were performed for the variable selection and the one with the smallest error was used. This resulted in 26 significant

Table 2

A schematic table showing the procedures of variable selection and calibration

Calibration series		Created models			
Measured	Predicted	MB1	MB2	MY1	MY2
B	B1	Test	Calibration	Calibration	Val/Cal
	B2	Calibration	Test	Val/Cal	Calibration
Y	Y1	Val/Cal	Calibration	Test	Calibration
	Y2	Calibration	Val/Cal	Calibration	Test

Val/Cal: validation set in the variable selection and calibration set in the calibration; Test: independent test set in calibration, excluded from variable selection; Calibration: calibration set in both variable selection and calibration.

Table 3

Error of prediction from calibration models with different data preprocessing

Zero fill <sup>a</sup>	Wavelet <sup>b</sup>	Exponential function <sup>c</sup>	rmsep (root-mean-square error of prediction)/(ppm) weight 4-aminophenol per weight paracetamol				
			MB1	MB2	MY1	MY2	Mean
No	No	No	35.0	23.9	15.4	27.1	25.3
Yes	Yes	No	20.9	59.1	32.2	37.5	37.4
Yes	Yes	Yes	62.0 <sup>d</sup>	58.5 <sup>d</sup>	29.9 <sup>d</sup>	46.4	49.2

MB1 is the calibration model with B1 as an independent test set in both variable selection and calibration, etc. see Table 2.

<sup>a</sup> Zero filling of the FID.

<sup>b</sup> Wavelet compression with symlet 2 in one step.

<sup>c</sup> Line broadening of the FID.

<sup>d</sup> Y2 was used as a test set in the variable selection but also included in the calibration model, where the test set is given by the name of the model. This may give a slightly smaller error than if the test set had been the same in the model throughout.

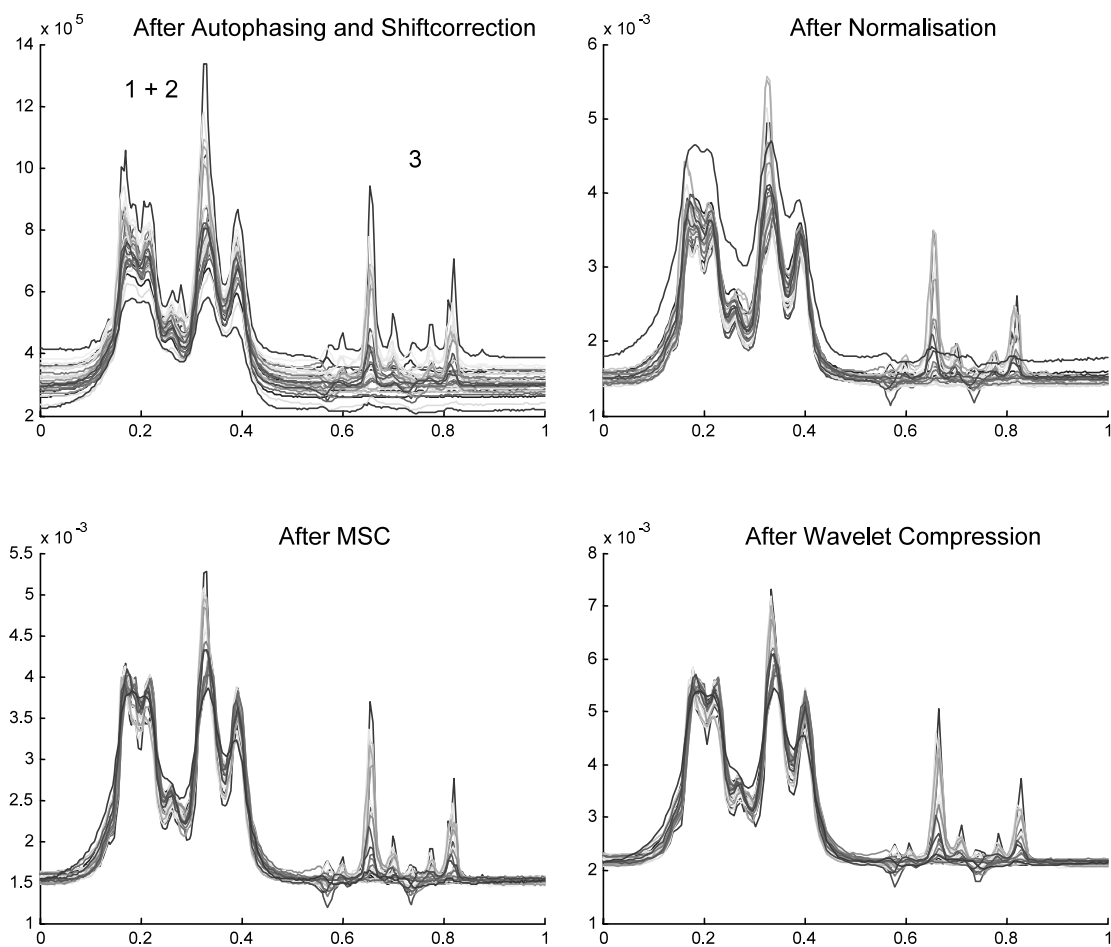


Fig. 2. The visible results from different data pre-treatments of the spectral area of interest, x-axis: 6.5–6.35 ppm; Autophasing and shift correction, normalisation, MSC and wavelet compression. The numbers in the spectrum at the upper left identify the numbered protons in Fig. 1. The spectra from all the calibration series (Y1, Y2, B1 and B2) are included.

wavelet variables based on the predetermined threshold. These were used for the NN building of the calibration model. The variables picked from the variable selection are illustrated in Fig. 3. The chosen variables all belong to the region in the spectral window that is expected to relate to the two substances studied.

The preprocessing of spectral data before the calibration model is built reduces the large quantity of information contained in an NMR spectrum, while preserving the relevant quantitative information. Autophasing, MSC and shift alignments were performed to minimize the dif-

ferences between spectra that did not correspond to concentration variations. However, from a Bayesian regularized NN perspective, due to computational constraints, the number of variables was too large (324), which meant that data compression had to be performed. The wavelet reduction of data (162 data points) and the variable selection reduce the number of variables further but preserves the information necessary for quantification. The relatively few (26) variables resulting make the building of the calibration models more rapid and give a more robust model.



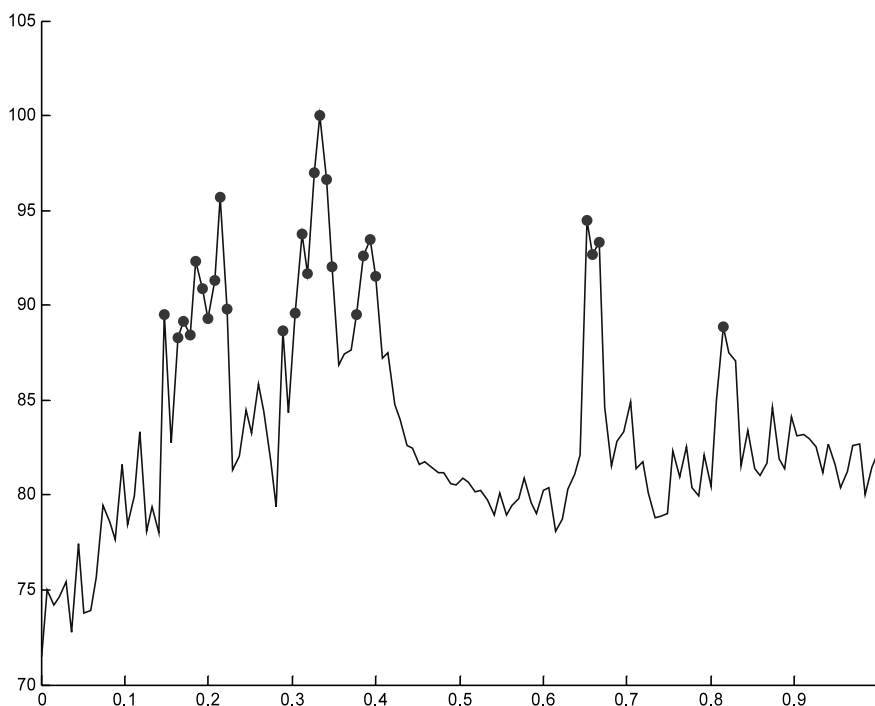


Fig. 3. Illustration of the variable selection. This is an example where Y2 is the test set and neither zero filling, line broadening nor wavelet compression are performed. The dots show the selected variables. *x*-Axis: 6.50–6.35 ppm, and *y*-axis: rmdiff [18].

#### 4.3. Calibration

The errors from the evaluation of each calibration model are shown in Table 3. For each test set, three independent calibration models were performed. The results were quite similar throughout each preprocessing condition, which indicates that the modelling is fairly robust. The mean rmsep of the final calibration model was  $25.3 \times 10^{-6}$  weight 4-aminophenol per weight paracetamol.

The mean rmsep in a molar relationship is  $35.0 \times 10^{-6}$  4-aminophenol/paracetamol. This is on the edge of what can be detected with the ADC sampling with 16 bits. Theoretically, the height of the smallest detectable peak is  $1/(2^{16}) = 15$  ppm (mole per mole). A peak twice as high corresponds to 30 ppm (mole per mole), which is really close to the mean error level from the resulting calibration models. These relatively small errors indicate that the preprocessing and reduction of data have been performed

without any loss of any quantitative information.

Plotting predicted versus measured data shows an obvious linear relationship, an example of

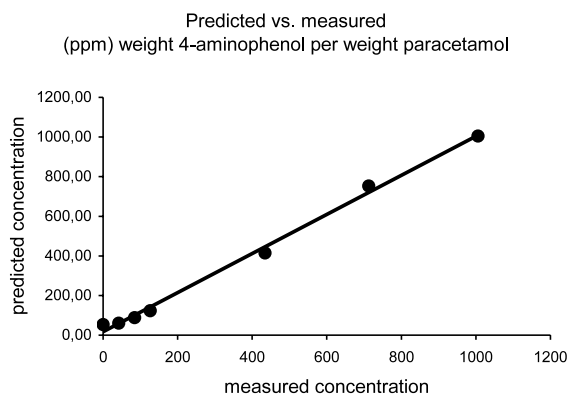


Fig. 4. Measured versus predicted concentrations from the final calibration model. This is an example where Y2 is the test set and neither zero filling, line broadening nor wavelet compression are performed. The equation for the line is  $y = 0.987x + 17.7$  and  $R^2 = 0.996$ .

which is shown in Fig. 4 with a slope of 0.99 and an intercept of 18 ppm (weight per weight). A statistical analysis of the linear fit shows that zero is included in the intercept with a confidence interval of 95%. This is true for all of the four models. The repeatability of these predictions was estimated by calculating the relative standard deviation (RSD), of predictions from the test sets at the same concentration level. In the middle of the concentration range, at 430 ppm (weight per weight), the RSD was 7.6%. This is a satisfying result in connection with impurity determination.

Although, the proposed scheme for preprocessing is somewhat complex, once developed it is readily applied for quantitative measurements. The combined affect of NMR analysis, preprocessing and NN regression of NMR data for analysing impurities is simple and relatively fast, about 20 min. The advantages of the method are that no pretreatment of the samples is needed (only dissolving), possible unknown impurities may be detected because of the selective spectrum and the analytes can easily be recycled if needed.

## 5. Conclusions

The results of this study indicate that QNMR in combination with multivariate methods has a potential for impurity determinations, not only for well-resolved NMR shifts but also for cases where a substantial peak overlap occurs. When peaks interfere with each other, nonlinear multivariate calibration methods may successfully be used. Since QNMR may have difficulties dealing with e.g. peak shift differences between spectra and base line drifts, the data preprocessing seems to be of great importance to abbreviate these phenomena. Common spectral preprocessing techniques such as MSC can substantially reduce some differences that are not dependent on the concentration variations. This study has also shown that some preprocessing of data that are intuitively known to improve the spectra does not improve the predictability in a quantitative study.

If the analyse time, i.e. the number of scans, had been increased, the  $S/N$  in the method would probably have been higher. However, this would

not perhaps have decreased the errors of the peaks utilized for integration according to the discussion above about the influence of the range of the ADC, which points to the importance of the dynamic range of the ADC used in QNMR.

An important advantage of QNMR is its direct applicability. Where other analytical methods include several steps of sample preparation, the NMR analysis most often merely requires the sample to be dissolved in a deuterated solvent. The ready availability nowadays of NMR instrumentation at even higher field strengths than 400 MHz and the rapid development of cryoprobes make QNMR a suitable alternative to conventional methods for impurity determinations.

## Acknowledgements

We are grateful to Susanne Olofsson and Anders Andersson, Department of Chemistry, AstraZeneca R&D Södertälje, for providing access to the NMR spectrometer and for valuable support regarding instrument aspects and theoretical NMR discussions.

## References

- [1] D.P. Hollis, *Anal. Chem.* 35 (1963) 1682–1684.
- [2] M.L. Anhoury, P. Crooy, R. De Neys, A. Laridant, *J. Pharm. Sci.* 65 (1976) 590–592.
- [3] I.K. O'Neill, M.A. Pringuer, H.J. Prosser, *J. Pharm. Pharmacol.* 27 (1975) 222–225.
- [4] M.H. Bowen, I.K. O'Neill, M.A. Pringuer, *Proc. Soc. Anal. Chem.* 11 (1974) 294–297.
- [5] F. Kasler, *Quantitative analysis by NMR spectroscopy*, in: F. Kasler (Ed.), *The Analysis of Organic Materials*, Academic, London, 1973, pp. 142–162.
- [6] B. Lindgren, *Pharmazie* 48 (1993) 51.
- [7] J.T.W.E. Vogels, J.C. Venekamp, *Profiling impurities in chlome-thiazole edisilate using proton NMR spectroscopy and multivariate calibration techniques*, TNO Nutrition and Food Research Institute, TNO Report/V97.659, Zeist (1997).
- [8] K.A.M. Thakur, R.T. Kean, E.S. Hall, M.A. Doscotch, E.J. Munson, *Anal. Chem.* 69 (1997) 4303–4309.
- [9] U. Holzgrabe, B.W.K. Diehl, I. Wawer, *J. Pharm. Biomed. Anal.* 17 (1998) 557–616.
- [10] P.P. Lankhorst, M.M. Poot, M.P.A. deLange, *Pharmacop Forum* 22 (1996) 2414–2422.
- [11] G. Maniara, K. Rajamoorthi, S. Rajan, G.W. Stockton, *Anal. Chem.* 70 (1998) 4921–4928.

- [12] P.M. Lacroix, B.A. Dawson, R.W. Sears, D.B. Black, T.D. Cyr, J.C. Ethier, *J. Pharm. Biomed. Anal.* 18 (1998) 383–402.
- [13] P. Fux, *Analyst* (Cambridge, UK) 115 (1990) 179–183.
- [14] L.S. Simeral, *Appl. Spectrosc.* 49 (1995) 400–402.
- [15] V. Ruiz-Calero, J. Saurina, M.T. Galceran, S. Hernandez-Cassou, L. Puignou, *Analyst* (Cambridge, UK) 125 (2000) 933–938.
- [16] L. Griffiths, *Analyst* (Cambridge, UK) 123 (1998) 1061–1068.
- [17] A.E. Derome, *Modern NMR Techniques for Chemistry Research*, Pergamon, Oxford, 1987.
- [18] F.O. Andersson, M. Aberg, S.P. Jacobsson, *Chemometrics Intelligent Lab. Syst.* 51 (2000) 61–72.
- [19] D.I. Hoult, R.E. Richards, *J. Magn. Reson.* 24 (1976) 71–85.
- [20] J.C. Lindon, J.K. Nicholson, I.D. Wilson, *Prog. Nucl. Magn. Reson. Spectrosc.* 29 (1996) 1–49.
- [21] D.D. Traficante, *Concepts Magn. Reson.* 4 (1992) 153–160.
- [22] M.M. Fuson, *J. Chem. Educ.* 71 (1994) 126–129.
- [23] D.L. Rabenstein, D.A. Keire, *Pract. Spectrosc.* 11 (1991) 323–369.
- [24] D.E. Goldberg, *Genetic Algorithms in Search, Optimization, and Machine Learning*, Addison-Wesley Publishing Company, Inc, 1989.
- [25] P. Geladi, D. MacDougall, H. Martens, *Appl. Spectrosc.* 39 (1985) 491–500.
- [26] I. Daubechies, *Ten lectures on wavelets*, in: *Society for Industrial and Applied Mathematics*, SIAM, Philadelphia, Pennsylvania, 1992.
- [27] M.T. Hagan, M. Menhaj, *IEEE Trans. Neural Networks* 5 (1994) 989–993.
- [28] P.E. Gill, W. Murray, M.H. Wright, *Practical Optimization*, Academic Press Inc, London, 1981.
- [29] F.D. Foresee, M.T. Hagan, “Gauss–Newton approximation to Bayesian regularization”, *Proceedings of the 1997 International Joint Conference on Neural Networks* (1997).
- [30] D.J.C. MacKay, *Neural Comput.* 4 (1992) 415–446.
- [31] MATLAB 5.3, The Mathworks, Natick, MA, USA.